ELSEVIER

S0032-3861(96)00373-4

Polymer Vol. 37 No. 22, pp. 4891–4907, 1996

0032-3861/96/$15.00+0.00

The role of matrix molecular weight in rubber toughened nylon 6 blends: 1. Morphology

A. J. Oshinski, H. Keskkula and D. R. Paul*
Department of Chemical Engineering, Center of Polymer Research, University of Texas at Austin, Austin, TX 78712, USA
(Received 21 August 1995)

The effects of polyamide molecular weight on morphology generation in nylon 6 blends with maleated elastomers are described. The elastomers used include styrene–butadiene–styrene block copolymers with a hydrogenated mid-block, SEBS, and versions with X% grafted maleic anhydride, SEBS-g-MA-X%, and an ethylene/propylene copolymer, EPR, and a maleated version EPR-g-MA. The molecular weight of the nylon 6 phase governs the melt viscosity of the blend matrix and the number of amine end groups available for reaction with the maleic anhydride groups in the rubber phase; both of which influence the size, shape, and size distribution of the rubber phase formed during blending. In general, rubber particle size, distribution, and the amount of occluded material in the rubber phase decreases as the nylon 6 molecular weight increases. Measurement of the extent of reaction between the amine end groups and the grafted maleic anhydride revealed that a higher fraction of nylon 6 chains are grafted to the rubber matrix as the nylon 6 molecular weight increases. The weight average rubber particle size and size distribution for blends based on SEBS-g-MA-X% are smaller than corresponding blends based on SEBS/SEBS-g-MA-2% mixtures containing the same amount of maleic anhydride. EPR/EPR-g-MA mixtures produce non-spherical morphologies that are typically larger and more polydisperse than SEBS type elastomers. One reason for this difference is the fact that SEBS elastomers react more readily with nylon 6 than do EPR/EPR-g-MA mixtures as determined by extent of amine reaction and torque rheometry. The weight average rubber particle size for blends of the various rubbers and nylon 6 materials were correlated using a modified Taylor theory analysis. A master curve was generated by determining shift factors needed to superimpose the maleated rubber/nylon 6 curves onto a reference curve for the non-maleated rubber, SEBS. The overall shift factors correlate linearly with the maleic anhydride content of the rubber phase. Copyright © 1996 Elsevier Science Ltd.

(Keywords: nylon 6; compatibilization; maleic anhydride)

INTRODUCTION

Numerous studies have been reported on the rubber toughening of polyamides using maleated rubbers[1–22]. The grafted maleic anhydride readily reacts with the polyamide amine end groups to give a graft copolymer which effectively controls the morphology and strengthens the interface between the two phases[13,14,21–25]. The result is a reduction in rubber particle size, mainly by a decrease in the particle–particle coalescence rate[4,26], and generally an improvement in mechanical toughness.

Rubber particle size has been shown to be critical for improving the toughness of these blends; prior studies indicate that to achieve super-toughness for polyamide matrices the rubber particle size must be below approximately 1 μm. However, rubber particles smaller than a lower limit of approximately 0.2 μm do not cause toughening of nylon 6[21,27]. Wu has proposed that the surface to surface distance between rubber particles rather than rubber particle diameter is the critical parameter controlling toughness; however, for a fixed rubber content, rubber particle size directly controls the interparticle distance[14].

Previous studies have focused mainly on how the nature of the rubber phase and factors that affect morphology generation, e.g. degree of maleation, processing parameters, relative melt viscosities of the two phases, etc., influence toughening[5,9,10,13,14,17,28,29]. Relatively little work has been reported on how the nature of the polyamide phase affects rubber toughening. Exceptions are recent studies that have compared morphology generation and toughening of nylon 6 and nylon 6,6[21,22], and more broadly nylon x and nylon x, y materials of varying x and y values using the same maleated rubber and processing procedures[4], plus an effort to examine the effect of matrix molecular weight by diluting a nylon 6/butadiene rubber blend with other nylon 6 materials of different molecular weight[20].

This series of papers[30,31] explores in some detail the effect that the molecular weight of nylon 6 plays in morphology generation and toughening of blends with maleated triblock and random copolymer rubbers. The triblock copolymers are hydrogenated styrene-butadiene-styrene elastomers whose mid-block resembles ethylene/butene copolymers, designated as SEBS, and versions grafted with various amounts of maleic anhydride, designated as SEBS-g-MA-X%. The

* To whom correspondence should be addressed

Table 1 Characterization of nylon 6 materials

Supplier's designation	$\bar{M}_n$[b]	$\bar{M}_n$[c]	[COOH] (μeq g^{-1})	[NH_2] (μeq g^{-1})	Brabender torque[d] (m − g)	Supplier
Capron XA-1767[a]	13 100	22 600	42.6	46.6	161	Allied Signal Inc.
Ultramid B0	13 200	13 200	74.2	77.0	175	BASF Corp.
Ultramid B1	14 900	14 000	70.2	72.5	260	BASF Corp.
Capron 8202	16 400	16 700	60.8	59.0	325	Allied Signal Inc.
Ultramid B3[a]	17 500	23 100	50.7	35.8	380	BASF Corp.
Ultramid B2	19 400	19 500	48.5	54.0	425	BASF Corp.
Capron 8207F	22 000	22 000	43.0	47.9	650	Allied Signal Inc.
Capron 8209F	29 300	31 400	28.8	34.8	1380	Allied Signal Inc.
Ultramid B5	37 300	38 600	23.8	28.1	1980	BASF Corp.

[a] Chain termination during polymerization using mono-amines and/or mono-acids
[b] From intrinsic viscosity measurements using $[\eta] = 5.26 \times 10^{-4} \bar{M}_w^{0.745}$ assuming $\bar{M}_n = 1/2\bar{M}_w$
[c] From end group analysis assembly only NH_2 or COOH groups at chain ends, i.e. $\bar{M}_n = 2/([NH_2] + [COOH])$
[d] Torque value taken after 10 min of mixing at 240°C and 60 rpm

Table 2 Rubbers used in this study

Designation used here	Material (supplier's designation)	Composition	Molecular weight	Brabender torque[a] (m − g)	Supplier
SEBS	Kraton G 1652	29% wt styrene	Styrene block = 7000 EB block = 37 500	1050	Shell Chemical Co.
SEBS-g-MA-0.5%	RP-6510	29% wt styrene 0.46% wt MA[b]	N/A	980	Shell Chemical Co.
SEBS-g-MA-1%	Kraton FG-1921X	29% wt styrene 0.96% wt MA[b]	N/A	815	Shell Chemical Co.
SEBS-g-MA-2%	Kraton FG-1901X	29% wt styrene 1.84% wt MA[b]	N/A	650	Shell Chemical Col.
L-SEBS	Kraton 1657	13% wt styrene	Styrene block = 5500 EB block = 73 000	N/A	Shell Chemical Co.
L-SEBS-g-MA	RP-6509	13% wt styrene 1.4% wt MA[b]	N/A	310	Shell Chemical Co.
EPR	Vistalon 457	43% wt ethylene 53% wt propylene	$\bar{M}_w = 54\,000$ $\bar{M}_w/\bar{M}_n = 2$	1450	Exxon Chemical Co.
EPR-g-MA	Exxelor 1803	43% wt ethylene 53% wt propylene 1.14% wt MA[b]	N/A	995	Exxon Chemical Co.

[a] Brabender torque taken after 10 min of mixing at 240°C and 60 rpm
[b] Determined by elemental analysis after solvent/non-solvent purification

random copolymers used in this study are maleated and non-maleated ethylene/propylene elastomers, designated as EPR-g-MA and EPR, respectively. The amount of maleation of the rubber phase was varied by dilution of a highly grafted rubber with its non-functionalized rubber counterpart or by the degree of grafting of maleic anhydride on the rubber backbone. This paper focuses on the morphology of the rubber phase (particle shape and size distribution) as a function of the rubber type (SEBS or EPR), the amount of maleation, and the molecular weight of the polyamide phase. The extent of reaction between the amine and maleic anhydride groups after melt processing is quantified and used to interpret morphological differences. An attempt to unify the effect of rheological properties, which for the polyamide matrix varies greatly with molecular weight, and grafted maleic anhydride content on rubber particle size is made using a modified Taylor theory analysis. Subsequent papers will focus on how particle size, polyamide molecular weight, and rubber type (SEBS or EPR) influence toughness at room temperature and the ductile brittle transition temperature.

EXPERIMENTAL

Table 1 provides information about the nine nylon 6 materials used in this work while *Table 2* describes the various rubbers. Nylon 6 is polymerized by ring-opening of caprolactam which normally yields chains with only one amine and one acid end group per molecule, i.e. balanced end groups. However, two of the polyamides (XA-1767 and B-3) employed monofunctional amines and acids during polymerization; a technique typically used to limit the molecular weight[32,33]. In such cases there will be non-reactive end groups and the number of amine and carboxyl end groups may not be balanced. In order to include low molecular weight materials with one amine and one carboxyl end per chain, three nylon 6 products were specially prepared for this study, Ultramid B0, B1, and B2. End group configuration has been shown in previous studies to influence the morphology generated during reactive extrusion with maleated rubbers[4,22,34]. Polyamides with difunctional character, chains with two amine groups on some chains, tend to form large, non-spherical rubber particles when compounded in a single screw extruder. The remaining polyamides were

not chemically modified and have one amine and one carboxyl group per chain.

Two fundamentally different types of rubbers were used in this study. One consists of triblock copolymers having styrene end blocks and a hydrogenated butadiene mid-block resembling an ethylene/butene copolymer, designated as SEBS. A series of such materials containing various amounts of maleic anhydride units grafted to the mid-block were used, designated here as SEBS-g-MA-X%, where X indicates the nominal content of grafted maleic anhydride. Three of the SEBS-g-MA-X% were made from the same nonfunctional precursor (SEBS). The melt viscosity (as indicated by Brabender torque rheometry) decreases in this series as the maleic anhydride content increases suggesting some chain scission occurs during maleation[35]. The triblock copolymer designated as L-SEBS-g-MA contains a higher molecular weight rubber mid-block and lower molecular weight styrene end blocks than the other block copolymers in *Table 2*. The other rubber type is a random ethylene/propylene copolymer (EPR) and a maleated version (EPR-g-MA). The maleated version also has a lower melt viscosity than the non-maleated precursor, EPR, once again suggesting chain scission occurs during grafting.

Prior to all melt processing steps, the polyamides were dried in a vacuum oven at 80°C for a minimum of 16 h. The rubbers were dried in a convection oven at 60°C.

Rheological properties of each material were assessed by torque rheometry using a Brabender Plasticorder operated at 240°C and 60 rpm with a 50 ml mixing bowl. Torque readings were measured continuously; however, the values reported were taken after 10 min of mixing. Viscoelastic properties of SEBS-g-MA-2% and EPR-g-MA in the melt were also determined with a Rheometrics Dynamic Analyzer RDA-2 at 240°C using a parallel plate configuration.

Blends were prepared using a Killion single screw extruder (L/D = 30 D = 2.54 cm) having an intensive mixing head operated at 240°C and 40 rpm.

The degree of maleation in the rubber phase was controlled using combinations of functionalized rubber and its precursor (designated as SEBS/SEBS-g-MA-2%) or using the SEBS-g-MA-X% series of rubbers. All blends were prepared by vigorously mixing all three compounds together at a ratio of 20% rubber with 80% nylon 6 prior to feeding into the extruder. The mixture was then extruded twice to ensure adequate mixing. EPR/EPR-g-MA rubber blends required an additional processing step prior to extrusion. The non-maleated EPR rubber was received in bale form, and cubes (2 cm × 2 cm) were cut from strips taken from the rubber block. These cubes were too large to feed into the extruder so a masterbatch of 50% EPR and 50% nylon 6 was prepared in a 250 ml Brabender Plasticorder and chopped into fine flakes (0.25 cm × 0.25 cm) before blending with additional nylon 6 and EPR-g-MA in the extruder. Blends were formed into standard tensile (ASTM D638 Type I) and Izod impact (ASTM D256), 0.318 cm thick, specimens using an Arburg Allrounder injection moulding machine.

Blend morphology was assessed via transmission electron microscopy (TEM) using ultra-thin sections cryogenically microtomed from Izod bars perpendicular to the flow direction. A Reichert-Jung Ultracut E microtome cooled to −45°C and equipped with a diamond knife was used to obtain the ultra-thin sections (20–50 nm thick). The sections were exposed to a 2% aqueous solution of phosphotungstic acid for 30 min to stain the polyamide phase. A JEOL 200 CX or a JEOL 1200 EX transmission electron microscope operating at 120 kV was used to view the specimens.

Rubber particle size analysis was done using a semi-automatic digital image analysis technique which employed IMAGE® software developed for the National Institutes of Health. The apparent diameter was determined by scanning the photomicrograph and individually outlining the particles to calculate the average of its longest dimension and the dimension perpendicular to the major axis. Typically over 200 particles and several fields of view were analysed. Because of the non-spherical nature of the particles, no corrections were applied to convert apparent particle diameters into true particle sizes[36–38]; although, the potential effects of this issue on the observed particle size distribution is discussed.

The acid and amine end group concentrations for each nylon 6 material and certain blends were determined using titration methods[39–48]. The acid concentration was analysed by dissolving the polyamide in benzyl alcohol at 110°C and titrating the hot solution to a phenolphthalein end point with 0.01 N KOH/benzyl alcohol. The amine concentration was determined by potentiometric titration, first by dissolving the polyamide in a 15/85 methanol/phenol solution for 48 h and determining the pH inflection point while adding a 0.01 N perchloric acid/methanol solution. Blends of nylon 6 and rubber were analysed for residual amine concentration as a means of determining extent of reaction, assuming the dominate reaction is between amine end groups and anhydride units to form image linkages[5,49]. Izod bars of the blends were cut into small pieces (0.5 cm × 0.5 cm), dried for 24 h at 60°C, and dissolved in a 15/85 methanol/phenol solution using high agitation for 48 h. The result is a viscous solution which can then be titrated in the same manner as neat nylon 6 with the exception that additional time must be given for the perchloric acid solution to react and allow the pH reading to stabilize. A more detailed description of the procedure is presented elsewhere[50].

Intrinsic viscosities were determined in a 100 ml Cannon-Fenske viscometer at 25°C using dilute solutions (<0.4 g dl^{-1}) of polyamide in *m*-cresol.

POLYAMIDE CHARACTERIZATION

The number average molecular weight of each nylon 6 material was calculated, see *Table 1*, from the results of end group analysis and intrinsic viscosity measurements with the assumptions outlined below. Numerous correlations between intrinsic viscosity and molecular weight have been developed[39–48]; however, the relation developed by Tuzar and Kratchovil[48] was found particularly useful for this work. They report

$$[\eta] = 5.26 \times 10^{-4} \bar{M}_w^{0.745} \quad (1)$$

for *m*-cresol as a solvent at 25°C.

Assuming that each sample has the most probable distribution, the values of $\bar{M}_n$ were calculated by dividing the $\bar{M}_w$ obtained from the intrinsic viscosity measurement, using equation (1), by two. If all end groups are

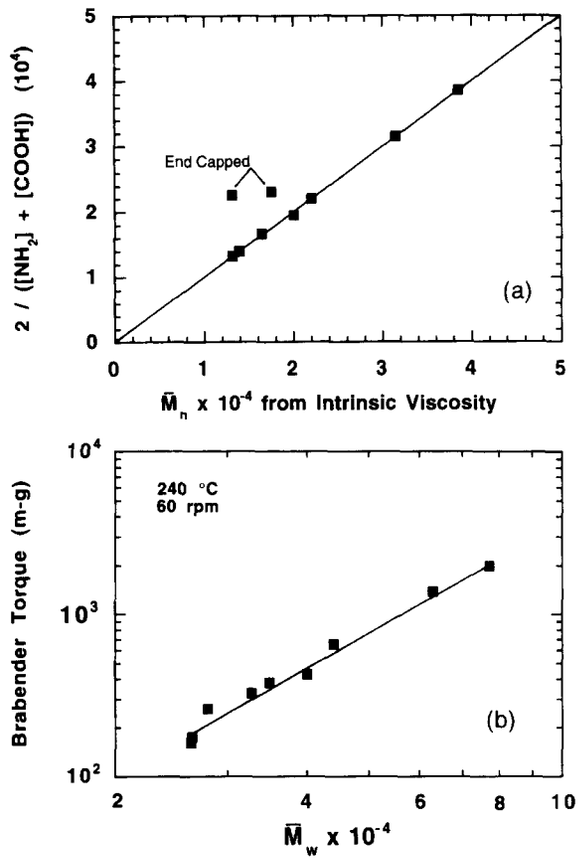

Figure 1 Characterization of nylon 6 materials in *Table 1*: (a) number average molecular weight determined by end group analysis *versus* that from intrinsic viscosity (see text for details); note that two end capped materials lie above expected line; (b) melt viscosity of nylon 6 as indicated by Brabender torque rheometry *versus* the weight average molecular weight determined from intrinsic viscosity measurements

either amine or acids, then the following applies

$$\bar{M}_n = 2/([NH_2] + [COOH]) \quad (2)$$

The values of $\bar{M}_n$ obtained from this relation are plotted vs the $\bar{M}_n$ from intrinsic viscosity in *Figure 1a*. The experimental data fall remarkably close to the theoretical 45° line except for the two end capped materials, Capron XA-1767 and Ultramid B3, which lie above the line since they have non-reactive end groups not counted in the titration procedure. The good agreement for the other materials provides evidence for the consistency of the assumed end group configuration, the assumed molecular weight distribution, and the experimental techniques used.

The Brabender torque values provide a measure of the melt viscosity for these materials. The torque is plotted vs the $\bar{M}_w$ from intrinsic viscosity in *Figure 1b* using logarithmic scales for both axes. The data fall along a straight line with slope equal to 2.3; this is less than the value of 3.4 expected for zero shear viscosity *versus* $\bar{M}_w$ suggesting that the effective shear rate in the Brabender experiment is well above the low shear limit for Newtonian behaviour[51].

QUANTITATIVE CHARACTERIZATION OF BLEND MORPHOLOGY

SEBS-g-MA-X%

Transmission electron microscopy (TEM) and image analysis were used to determine the effect of nylon 6 molecular weight and the maleic anhydride content of the rubber phase on the rubber particle size distribution. This section focuses on the SEBS-g-MA-*X*% materials while results for the rubber mixtures, SEBS/SEBS-g-MA-2% and EPR-EPR-g-MA, will be discussed and compared to these results later. Only three commercial SEBS-g-MA-*X*%, 0.5, 1, 1.84% MA, elastomers were available, and all three were made from the same non-maleated precursor, SEBS.

Figure 2 shows TEM photomicrographs for blends of SEBS and the maleated SEBS-g-MA-*X*% elastomers with two nylon 6 materials in *Table 1*, without chemical modification during synthesis, having the lowest (B0) and highest (B5) molecular weights. The rubber phase appears as white, semispherical domains within the dark polyamide matrix. The rubber particles progress from large, non-spherical particles containing occluded nylon 6 when the maleic anhydride content is low to small, spherically shaped particles with low amounts of occluded matrix material at high maleic anhydride contents. As the nylon 6 molecular weight increases, both the rubber particle size and amount of occluded material are reduced. The distribution of the rubber particle size appears to become more narrow as nylon 6 molecular weight increases, which is best demonstrated by the use of cumulative distribution plots for these blends.

Particle size distribution is displayed here as the cumulative fraction of particles at or below a specific size, on a log-normal distribution plot. A Gaussian distribution of particles would appear as a straight line with the number average particle size at 50% and the standard deviation inversely proportional to the slope. A steep slope indicates a narrow distribution; a monodisperse distribution would be a vertical line. Curvature indicates deviation from the Gaussian form and generally reflects skewness in the distribution. A bimodal distribution would appear as two straight line regions, if both populations are Gaussian, whose offset and slopes reflect the means and standard deviations of the two populations. In the present cases, cumulative distributions that depart from a simple straight line generally indicate a tendency towards bimodality.

Dimensional information regarding the rubber particle size was determined from TEM analysis of ultra-thin sections (20–50 nm thick) taken from injection moulded specimens. These ultra-thin sections actually represent random, parallel cuts through individual rubber particles as shown schematically in *Figure 3*. The effect of the section thickness relative to the actual diameter of the particle can contribute to the polydispersity trends revealed in cumulative distribution plots. When the particles are large relative to the section thickness (Δh), these cuts will rarely be through the equator of the particle so rather than revealing the actual diameter (D), an apparent diameter (d) is observed and it is this quantity that is actually used in the cumulative distribution plots. *Figure 3* shows the effect of the actual particle size relative to the section thickness on the apparent cumulative distribution curve for monodisperse particles that are randomly distributed within a matrix. The details of this calculation are presented elsewhere[50]. If the section thickness is constant, then for very small particles (where $\Delta h \sim D$) the cumulative distribution plot is free of the random cut effect as indicated by the vertical line. For large particles ($D \gg \Delta h$), this effect becomes significant such that the

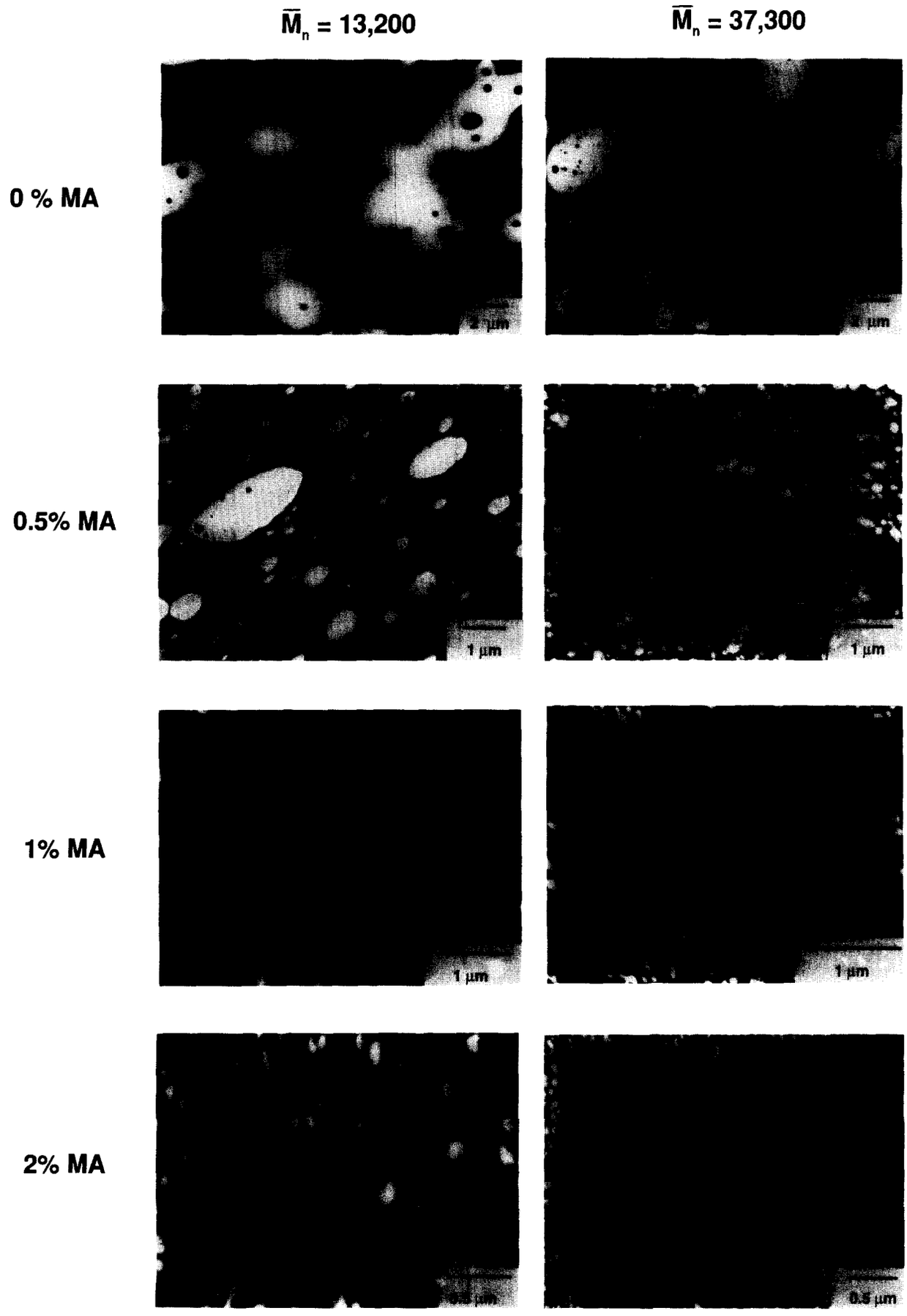

Figure 2 TEM photomicrographs of 20% SEBS-g-MA-X %/80% nylon 6 blends as a function of the content of maleic anhydride (X) and nylon 6 molecular weight: X = 0, 0.5, 1, and 2% and $\bar{M}_n$ = 13 200 and 37 300. The polyamide phase is stained dark with phosphotungstic acid

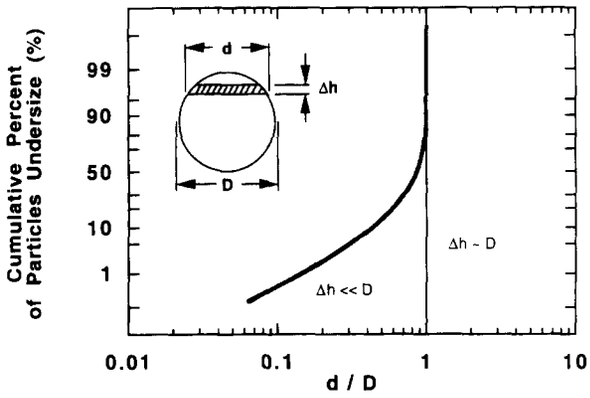

Figure 3 Illustration of how thin, $\Delta h \ll D$, random cuts by a microtome through monodisperse spheres of diameter D will seem to have a distribution of apparent particle diameters d when viewed by TEM. When the microtome cuts are comparable in thickness to the particle diameter D, the true monodisperse character of these particles will be seen in TEM photomicrographs

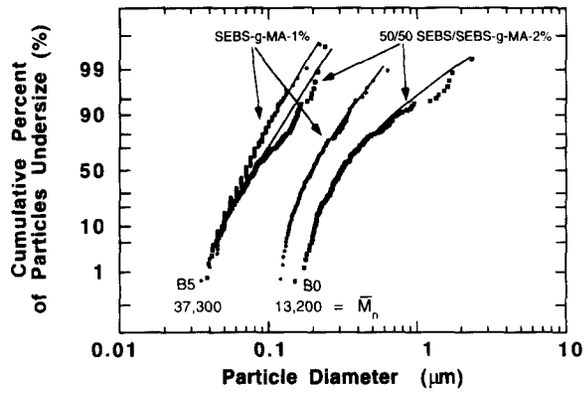

Figure 4 Cumulative apparent particle size distributions for 20% SEBS-g-MA-1% and 20% 50/50 SEBS-SEBS-g-MA-2% blends with 80% nylon 6 materials having number average molecular weights of 13 200 and 37 300. The two rubber systems being compared contain approximately 1% maleic anhydride by weight

distribution curve now contains a considerable number of apparent diameters that are smaller than the actual particle diameter before approaching the actual particle diameter in a vertical, asymptotic manner. For blends that contain a distribution of particle sizes, the upturn at the end of the calculated cumulative distribution curve may not be observed. Based on the section thickness used in this study, blends that have an average rubber particle size below approximately 0.1 μm should result in cumulative distribution plots free of the random cut effect.

From TEM photomicrographs like those in *Figure 2c* cumulative distribution plots were generated for blends of SEBS-g-MA-1% with nylon 6 materials of different molecular weights, see for example *Figure 4*. For the highest molecular weight nylon 6, B5, the line that best represents the data is relatively straight and has a steep slope, indicating that the rubber particle size distribution is narrow and unimodal. Conversely, for the blends based on the lowest molecular weight nylon 6, B0, the rubber particles are much larger and the sizes are broader and skewed as evidenced by the non-linear plot. The effects illustrated in *Figure 3* contribute more to the distribution of sizes for blends based on B0 than for the B5 type nylon 6.

From the particle size distribution, number, weight, and volume average diameters were calculated from the

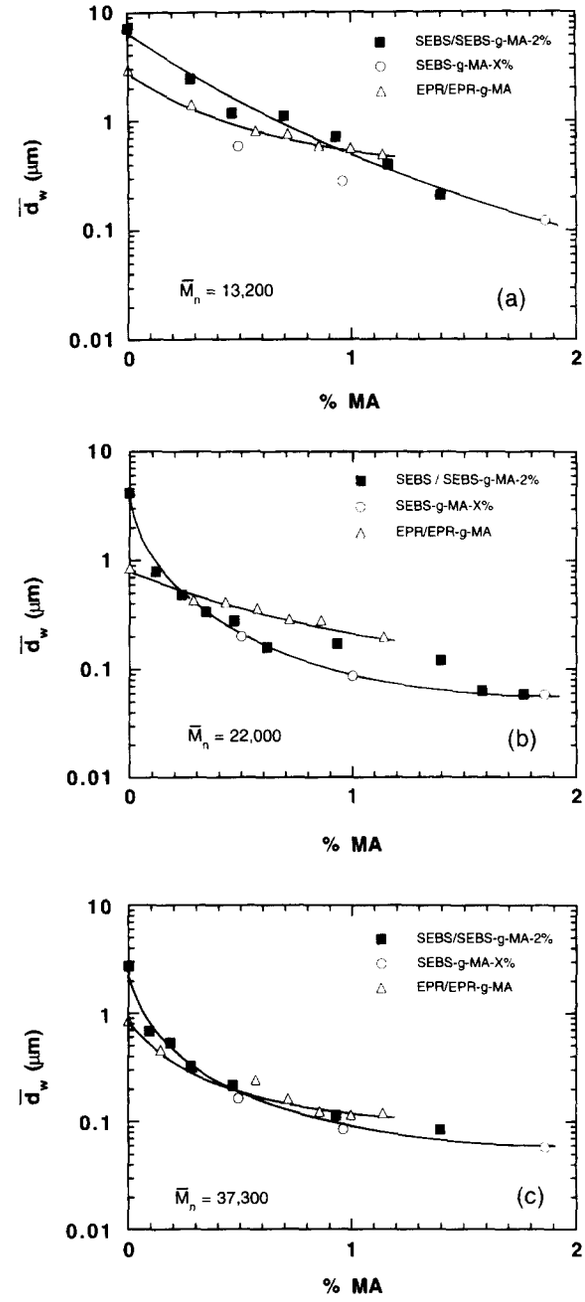

Figure 5 Effect of maleic anhydride content in rubber on weight average rubber particle diameter for blends of SEBS/SEBS-g-MA-2%, SEBS-g-MA-X %, and EPR/EPR-g-MA with nylon 6, all in the ratios 20% rubber/80% nylon 6. The nylon 6 molecular weight in each graph is as follows: (a) $\bar{M}_n$ = 13 200, (b) $\bar{M}_n$ = 22 000 and (c) $\bar{M}_n$ = 37 300

following relationships:

$$\bar{d}_n = \sum n_i d_i / \sum n_i \quad (3)$$

$$\bar{d}_w = \sum n_i d_i^2 / \sum n_i d_i \quad (4)$$

$$\bar{d}_v = \sum n_i d_i^4 / \sum n_i d_i^3 \quad (5)$$

where n_i is the number of rubber particles within the diameter range i[29,37,52,53]. All subsequent reference to rubber particle size will be the weight average diameter, $\bar{d}_w$, since this average is frequently used in correlations with toughness and because it gives a good representation of the trends reported here. The weight average rubber particle sizes for blends of the various SEBS-g-MA-X% elastomers (open circles) with nylon 6 materials having high (B5), low (B0), and medium (8207F) molecular weight are plotted in *Figure 5 versus*

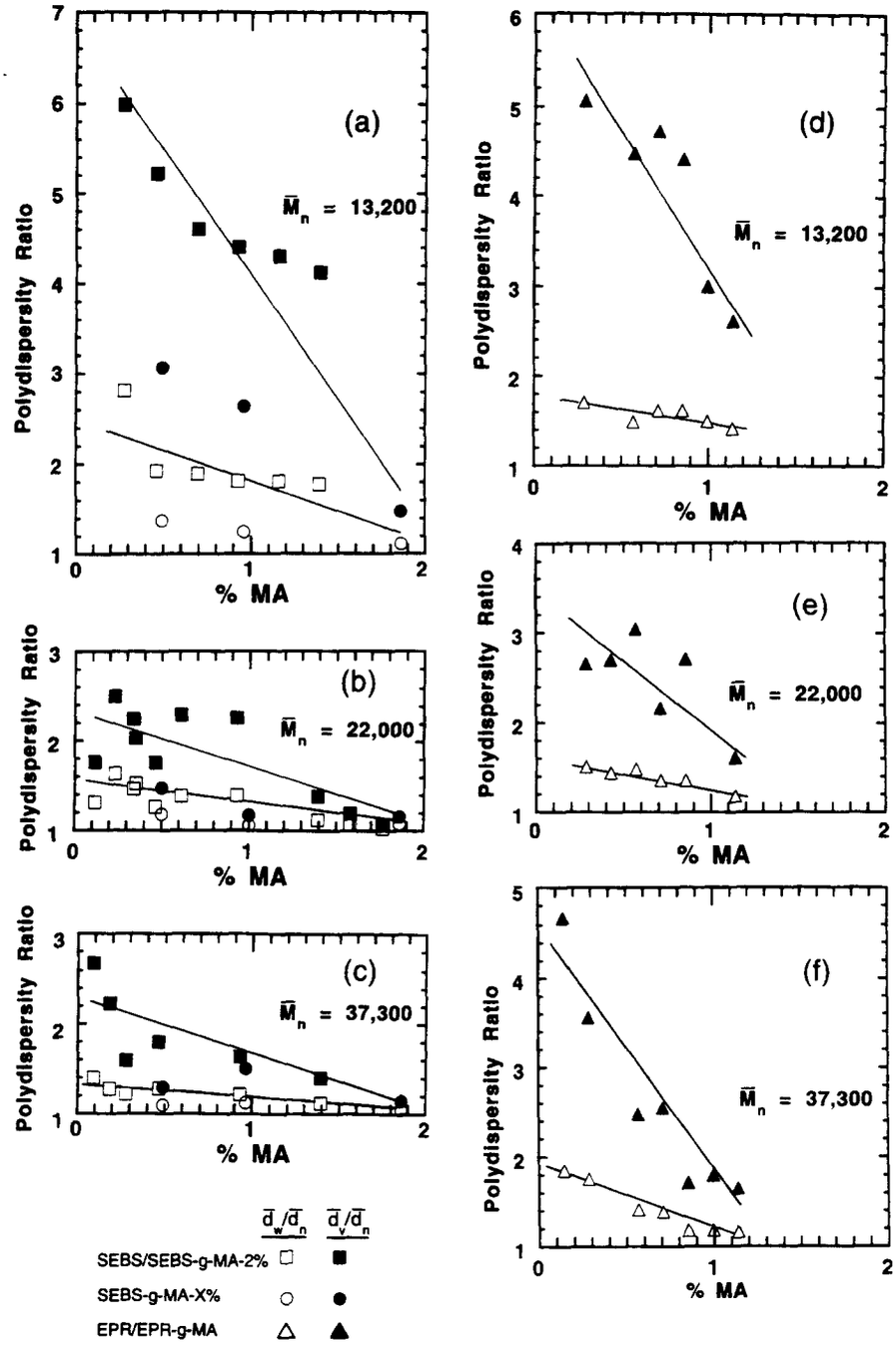

Figure 6 Effect of maleic anhydride content on the polydispersity of rubber particle sizes for blends of SEBS-g-MA-*X* % and SEBS/SEBS-g-MA-2% with nylon 6 materials having the following molecular weights: (a) $\bar{M}_n$ = 13 200, (b) $\bar{M}_n$ = 22 000 and (c) $\bar{M}_n$ = 37 300; and of EPR/EPR-g-MA with nylon 6 of these molecular weights: (d) $\bar{M}_n$ = 13 200, (e) $\bar{M}_n$ = 22 000 and (f) $\bar{M}_n$ = 37 300. All blends are 20% rubber/80% nylon 6

the degree of maleation. For each nylon 6 material, the particle size decreased approximately two orders of magnitude as the maleic anhydride content increases from 0 to 1.84%. Measures of particle size polydispersity, $\bar{d}_w/\bar{d}_n$ and $\bar{d}_v/\bar{d}_n$, are shown in *Figure 6* vs the maleic anhydride content. These ratios, represented by the open and closed circles, steadily decrease as the maleic anhydride content of the SEBS-g-MA-*X* % elastomers increases. For a given maleic anhydride content, the polydispersity appears to also decrease as the molecular weight of the nylon 6 matrix phase increases.

It is important to recall that TEM photomicrographs under typical circumstances only provide apparent particle diameters for the reasons illustrated in *Figure 3*. It is important to see the extent to which this effect influences the various average particle diameters and measures of polydispersity introduced above. For thin random cuts through monodisperse particles of diameter D, the distribution functions shown in *Figure 3* lead to

$$\bar{d}_n/D = 0.786 \quad (6)$$

$$\bar{d}_w/D = 0.849 \quad (7)$$

$$\bar{d}_v/D = 0.905 \quad (8)$$

The ratio given by equation (6) agrees well with the factor $\pi/4$ quoted in the literature[36–38]. For the weight and volume averages, the average apparent diameters are even closer to the true diameter, D. The polydispersity ratios given by these relations are $\bar{d}_w/\bar{d}_n = 1.08$ and $\bar{d}_v/\bar{d}_n = 1.333$. The polydispersity

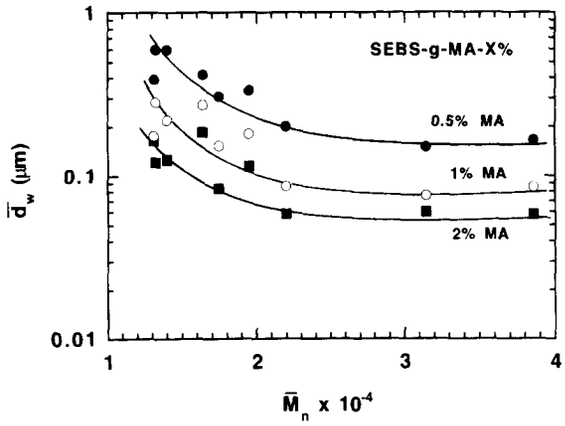

Figure 7 Weight average rubber particle diameter of 20% SEBS-g-MA-X%/80% nylon blends for $X = 0.5$, 1, and 2% as a function of nylon 6 molecular weight

ratios shown in *Figure 6* are generally much larger than these limits, indicating they are good measures of true polydispersity of particle sizes, except at high maleic anhydride contents where the particle diameters are very small and begin to approach more nearly the section thickness Δh and this effect no longer exists. Thus, it is concluded that these results reflect to a large degree true particle size distribution effects rather than apparent distributions stemming from the issue in *Figure 3*.

As seen in *Figure 7*, the weight average rubber particle size decreases as the nylon 6 molecular weight increases for each of the three SEBS-g-MA-X% elastomers but tends to reach a plateau at high levels of molecular weight. The rubber particle size decreases by more than 70% in going from the lowest to the highest molecular weight nylon 6 investigated in this study.

SEBS/SEBS-g-MA-2%

An alternative method of varying the amount of maleic anhydride in the rubber phase is to combine SEBS with SEBS-g-MA-2% in various ratios. Using this technique allows for finer control of the maleic anhydride content in the rubber phase than is possible with the limited series of SEBS-g-MA-X% elastomers discussed above. Earlier papers[21,54] suggest that mixing a non-functional SEBS with one of high grafted maleic anhydride content produces behaviour similar to uniformly grafted materials of the same maleic anhydride content. Indeed, the weight average rubber particle diameters for blends of nylon 6 with SEBS-SEBS-g-MA-2% mixtures and the SEBS-g- MA-X% materials follow the same general trend as a function of rubber phase maleic anhydride content as may be seen in *Figure 5*. This response implies that the functional and non-functional matrix mix to form a single rubber phase rather than two populations of particles generated from the two types of rubber.

A closer comparison of the two approaches to varying the degree of maleation is provided here. *Figure 8* shows TEM photomicrographs of blends of nylon 6 at the extremes of molecular weight with SEBS/SEBS-g-MA-2% mixtures and the SEBS-g-MA-X% materials where the maleic anhydride content is either 0.5 or 1%. Increasing the anhydride content reduces the rubber particle size for both types of elastomers, but the rubber particles in the blends based on the SEBS-SEBS-g-MA-2% mixtures do not appear as small or as well dispersed as those on the SEBS-g-MA-X% materials. It also appears that the amount of occluded nylon 6 in the rubber phase is greater in the case of the SEBS/SEBS-g-MA-2% mixtures.

Visual inspection of TEM photomicrographs like those in *Figure 8* for the SEBS/SEBS-g-MA-2% blends suggests a bimodal particle distribution in some cases for blends based on the low molecular weight nylon 6, B0. A quantitative analysis of the rubber particle size distribution for this nylon 6 blended with various ratios of SEBS-g-MA-2% (wt%) and SEBS is shown in *Figure 9*. The cumulative distribution plots are highly curved with evidence of bimodality, as discussed earlier, except when the rubber phase contains large amounts of SEBS-g-MA-2%. The remaining curves show very broad particle size distributions without distinct evidence of bimodality. All nylon 6 materials having molecular weights of 16 000 g mol^{-1} or less tend to show some tendency for bimodality when the SEBS/SEBS-g-MA-2% mixture has a low maleic anhydride content[50]. A prerequisite to forming a single population of particles under any circumstance would seem to require that the functionalized and non-functional elastomers must be miscible with each other which is not always assured. Recent work[55] has suggested that polypropylene, PP, is not miscible with maleated polypropylene, PP-g-MA, when the latter material contains more than 1% MA. When phase separated PP and PP-g-MA mixtures are blended with nylon 6, the polypropylene particles form two very distinct populations, one similar to that of PP and one similar to that of PP-g-MA. In general, the results shown here clearly support a mixed rubber phase rather than two populations of particles stemming from separate SEBS and SEBS-g-MA-2% phases, i.e. lack of miscibility, with the exception of blends of a rubber mixture with low maleic anhydride content with a low molecular weight nylon 6. In the latter case, the distribution of sizes is considerably broadened but there are no particles of the size expected for a pure SEBS phase. The low viscosity melt matrix produced by low molecular weight nylon 6 does not generate the high stress levels during mixing needed to break up large rubber particles. When the fraction of non-functional rubber is high, it is easy to understand that the SEBS-g-MA-2% may react with the polyamide matrix to form small particles before the excess of SEBS can be uniformly distributed within the small particles during the short residence time in the extruder. Therefore, the morphology that is observed appears to be a problem of insufficient mixing, not an inherent feature of the rubber mixture system and could possibly be improved by higher intensity mixing in a twin screw extruder.

Figure 4 compares the rubber particle size distribution for blends of the two SEBS type rubber systems containing 1% MA with high and low molecular weight nylon 6 materials. In both cases, the rubber particles are larger and have broader distribution of sizes in the case of the SEBS/SEBS-g-MA-2% mixture compared to SEBS-g-MA-1%; however, the differences are smaller for the high molecular weight nylon 6. The higher stress levels generated with the higher molecular weight nylon 6 material is capable of overcoming some of the difficulties of mixing with the SEBS-SEBS-g-MA-2%

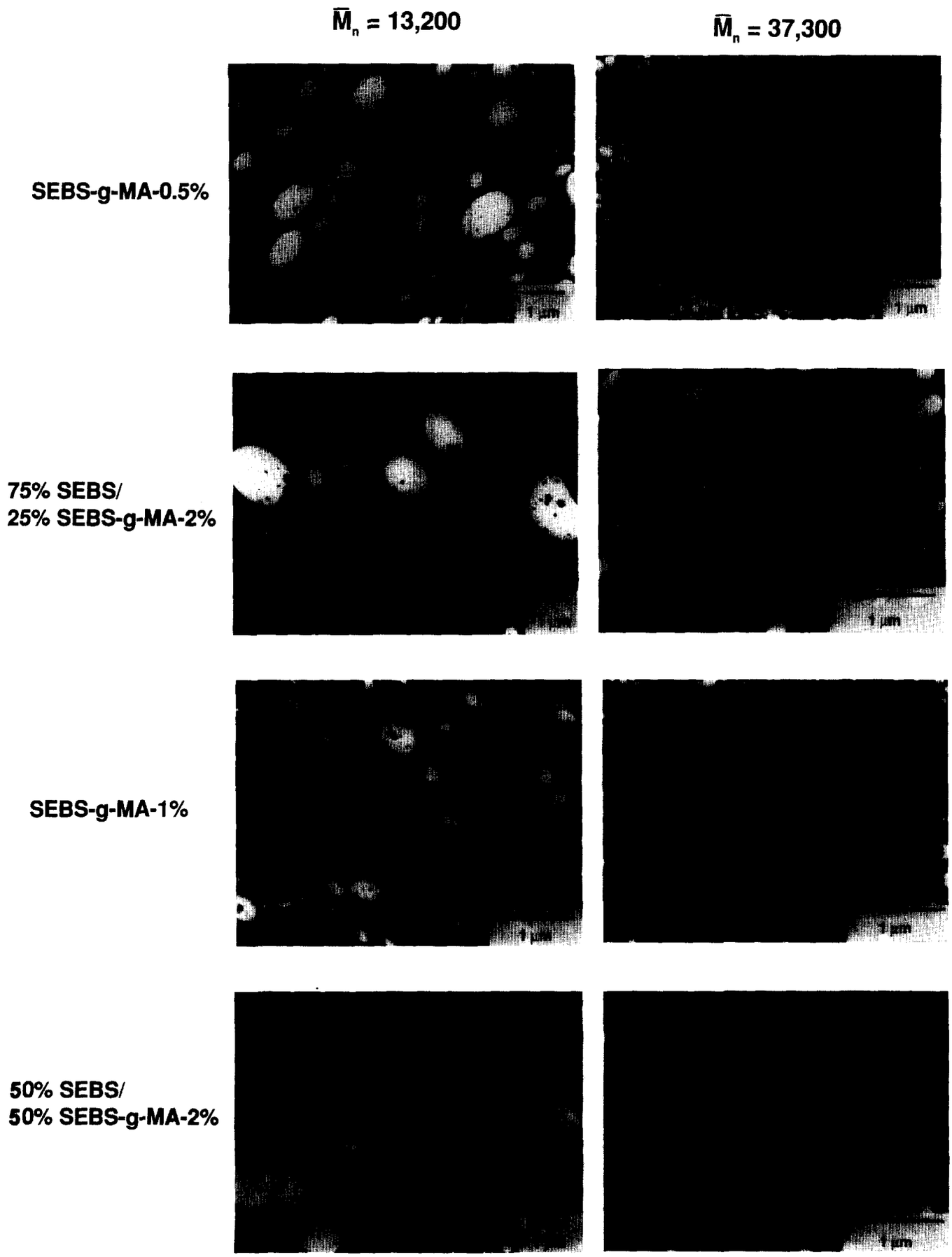

Figure 8 TEM photomicrographs of 20% SEBS-g-MA-X%/80% nylon 6 blends as a function of X and nylon 6 molecular weight: X = 0.5 and 1%, $\bar{M}_n$ = 13 200 and 37 300; and for 20% SEBS/SEBS-g-MA-2%/80% nylon 6 blends as a function of per cent SEBS-g-MA-2% and nylon 6 molecular weight: 25% and 50% SEBS-g-MA-2%, $\bar{M}_n$ = 13 200 and 37 300. Nylon 6 phase stained dark with phosphotungstic acid

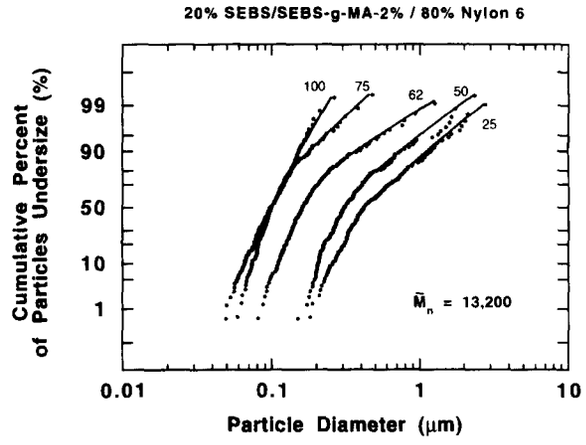

Figure 9 Cumulative particle size distribution plots for blends of 20% SEBS/SEBS-g-MA-2% with 80% nylon 6 ($\bar{M}_n$ = 13 200) where the SEBS-g-MA-2% percentage of the rubber phase is varied

mixture to produce both smaller particle sizes and narrower distributions.

While the weight average particle size for SEBS/SEBS-g-MA-2% mixtures and SEBS-g-MA-*X*% materials in nylon 6 blends follow the same trends (as seen in *Figure 5*), it is clear that the mixture of the two rubbers leads to a broader particle size distribution. *Figures 6a–c* clearly show this by comparing plots of the polydispersity ratios, $\bar{d}_v/\bar{d}_n$ and $\bar{d}_w/\bar{d}_n$, vs maleic anhydride content for three nylon 6 matrices. In all cases, these indicators of polydispersity decrease with increasing maleic anhydride content and nylon 6 molecular weight; however, the SEBS/SEBS-g-MA-2% mixtures (open and closed squares) have significantly greater values of these ratios than the SEBS-g-MA-*X*% elastomers (open and closed circles). For the lowest molecular weight nylon 6 (*Figure 6a*), the much larger polydispersity ratios at low maleic anhydride content are probably related to the mixing issues described above.

EPR/EPR-g-MA

Mixtures of a maleated ethylene/propylene rubber containing 1.14% MA, EPR-g-MA, and the non-maleated EPR precursor were blended with three nylon 6 materials having low (B0), medium (8207F), and high (B5) molecular weights. By varying the ratio of the nonfunctional to the functionalized rubber, the maleic anhydride content could be varied between 0 and 1.14%. As mentioned earlier, it was necessary to form a masterbatch of 50% EPR and 50% nylon 6 in a Brabender Plasticorder in order to add the non-maleated EPR to the extruder. This additional processing step increased the mixing history of the blend and may improve the dispersion of the EPR in the final blend with EPR-g-MA, especially for the low maleic anhydride content blends. An assessment of the effect of this additional processing step on blend morphology and properties was made by comparing blends generated from a similar masterbatch of 50% SEBS/50% nylon 6 (8207F) with those produced by simultaneously extruding all three components in one step. It was found that predispersing the non-maleated SEBS in nylon 6 reduced the weight average particle size and polydispersity approximately 10–15% for a composition based on a SEBS/SEBS-g-MA-2% mixture at 1% MA content; further details of these experiments and the mechanical properties of the resulting blends are given elsewhere[50]. The differences observed are about at the limit of the experimental reproducibility; however, at lower maleic anhydride contents more masterbatch material is used to produce the blends and may affect the particle size to a greater extent. It is important to keep this in mind when comparing the EPR/EPR-g-MA, SEBS-g-MA-*X*% and SEBS/SEBS-g-MA-2% rubber systems.

Figure 10 compares TEM photomicrographs of blends based on EPR-g-MA (1.14% MA) and SEBS-g-MA-1%; the maleic anhydride content and melt viscosity of the two rubbers are rather similar. The EPR-g-MA forms large, non-spherical, and highly occluded particles in both the low and high molecular weight nylon 6 matrices shown. Increasing the molecular weight of the matrix reduces the rubber particle size and the amount of nylon 6 occluded in the EPR-g-MA phase; both the average size and the size distribution of the rubber particles appear to be significantly larger for EPR-g-MA than for SEBS-g-MA-1%. A comparison of rubber particle sizes for the two rubber types is shown in *Figure 11* as a function of the polyamide molecular weight. It is obvious that the rubber particle size is significantly larger for EPR-g-MA than SEBS-g-MA-1%, even though the former has a slightly higher maleic anhydride content than the latter, regardless of the nylon 6 molecular weight. The quantitative comparison of particle size distribution, from photomicrographs like those in *Figure 10*, in *Figure 12* using cumulative distribution plots also shows greater polydispersity for EPR-g-MA than SEBS-g-MA-1% for both low and high molecular weight nylon 6 matrices. A discussion of factors that may be responsible for these differences in rubber particle size will be addressed later.

Figure 5 compares the weight average rubber particle size of EPR/EPR-g-MA mixtures in three nylon 6 matrices with the other rubber systems described above. The particles formed from EPR/EPR-g-MA mixtures are slightly smaller at low maleic anhydride contents than those formed from SEBS type elastomers, but as the maleic anhydride content increases the latter type particles are smaller. The polydispersity ratios are compared in *Figure 6*. In all cases, the particle size distribution becomes more narrow as the maleic anhydride content increases; however, at the same maleic anhydride content, the particles formed from SEBS/SEBS-g-MA-2% mixtures are less polydisperse than those from EPR/EPR-g-MA mixtures, except for the lowest molecular weight nylon 6. As noted earlier, rubber particles formed from SEBS/SEBS-g-MA-2% mixtures tend to show bimodality in very low molecular weight nylon 6 matrices; whereas, the same type blends based on EPR/EPR-g-MA mixtures generate small rubber particles with no evidence of bimodality. The polydispersity ratios for the EPR/EPR-g-MA system described here are similar to other reported values[18,27,56–58].

L-SEBS-g-MA

Figure 13 compares the size of the rubber particles formed by the L-SEBS-g-MA rubber and an SEBS/SEBS-g-MA-2% mixture of the same maleic anhydride content as a function of the nylon 6 molecular weight. L-SEBS-g-MA produces slightly smaller particles, but otherwise the trends are identical. This difference in size may be the result of the fact that the melt viscosity of the

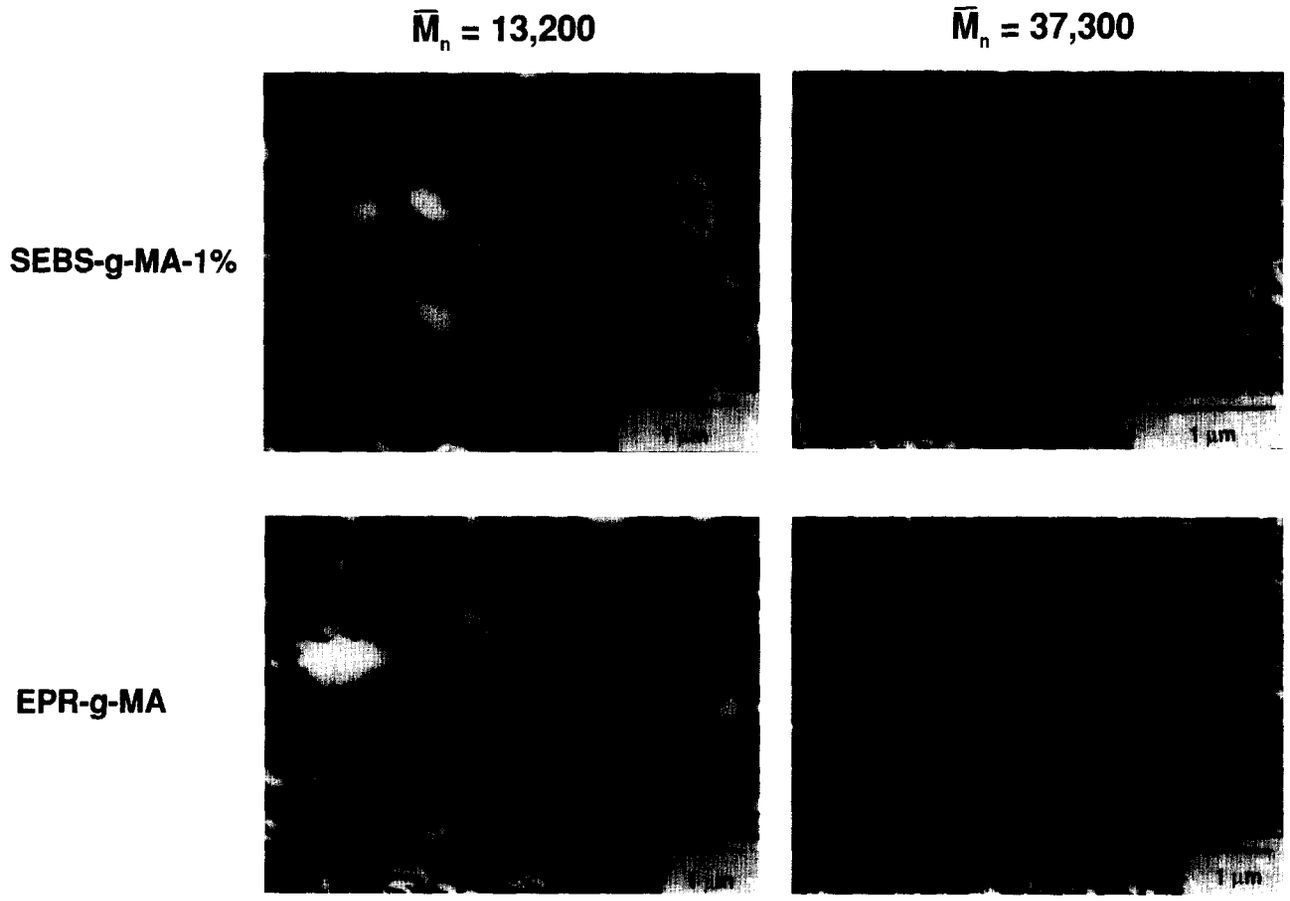

Figure 10 TEM photomicrographs for 20% SEBS-g-MA-1%/80% nylon 6 blends and 20% EPR-g-MA/80% nylon 6 where the nylon 6 molecular weight is 13 200 and 37 300. Nylon 6 phase is stained dark with phosphotungstic acid

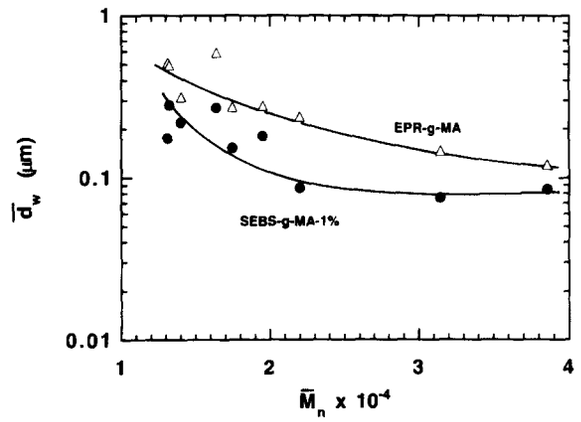

Figure 11 Effect of nylon 6 molecular weight on weight average rubber particle diameter for blends of 20% SEBS-g-MA-1%/80% nylon 6 and 20% EPR-g-MA/80% nylon 6. Note that both rubbers contain approximately 1% maleic anhydride by weight

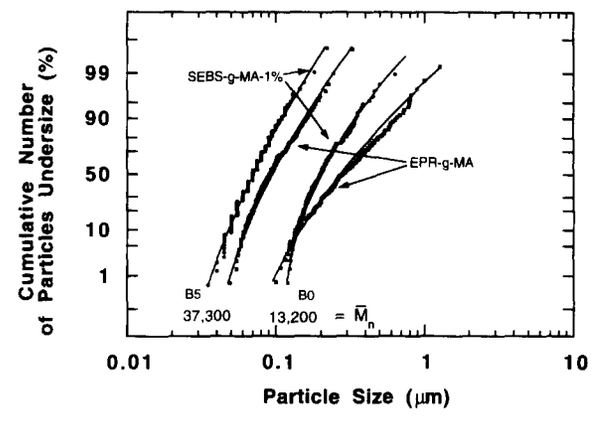

Figure 12 Cumulative particle size distribution plots for blends of 20% SEBS-g-MA-1%/80% nylon 6 and 20% EPR-g-MA/80% nylon 6 for nylon 6 materials of $\bar{M}_n$ = 13 200 and 37 300

L-SEBS-g-MA is approximately 2.5 times less than that of the 25% SEBS/75% SEBS-g-MA-2% mixture. As seen later, the extents of reaction between these two rubbers and nylon 6 are nearly identical.

EFFECT OF RUBBER TYPE ON BLEND MORPHOLOGY

From the TEM photomicrographs in *Figure 5* and the quantitative results shown in *Figures 10–12*, it is clear that the EPR and SEBS type elastomer systems lead to rather different morphological responses when blended with nylon 6 materials in a single screw extruder. Even when the maleic anhydride content and viscosities of the two rubber types are the same, the rubber particle sizes are significantly different as may be seen in *Figure 11*. The fact that EPR/EPR-g-MA mixtures tend to produce larger and more polydisperse particles than the SEBS elastomers, at maleic anhydride contents of 0.5% or greater, might be attributed to differences in the rheological characteristics of the two rubbers (viscosity or elasticity), interfacial characteristics of the polyamide-rubber pair, or to the ability of grafted maleic anhydride to react and promote compatibilization with the nylon 6 matrix. This section explores the potential differences in

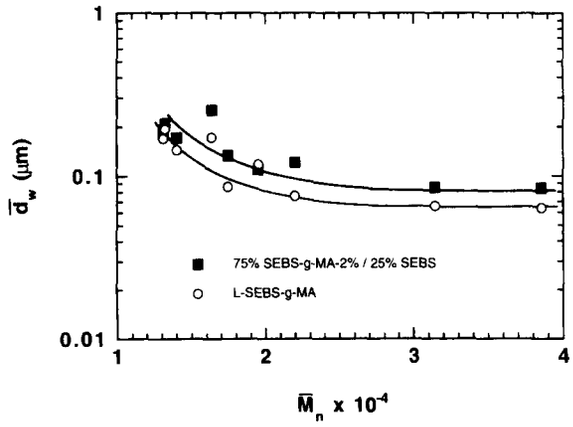

Figure 13 Effect of nylon 6 molecular weight on weight average rubber particle diameter for blends of 20% L-SEBS-g-MA/80% nylon 6 and 20% (75% SEBS-g-MA-2%/25% SEBS)/80% nylon 6. Note that the maleic anhydride content of both rubber systems is constant at ~1.4%

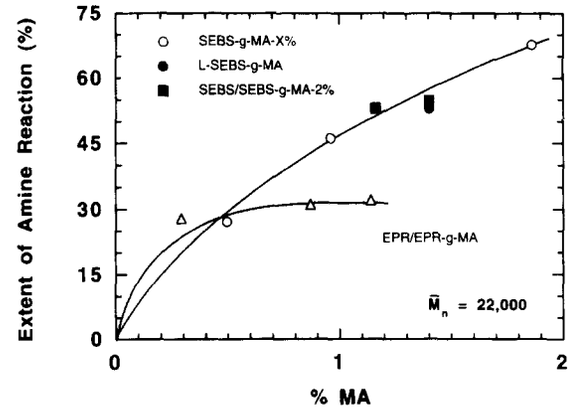

Figure 15 Effect of maleic anhydride content of the rubber phase on the extent of amine reaction in 20% rubber/80% nylon 6 ($\bar{M}_n$ = 22000) blends, for the rubbers EPR/EPR-g-MA, SEBS/SEBS-g-MA-2%, SEBS-g-MA-*X*%, and L-SEBS-g-MA, following melt compounding and injection moulding

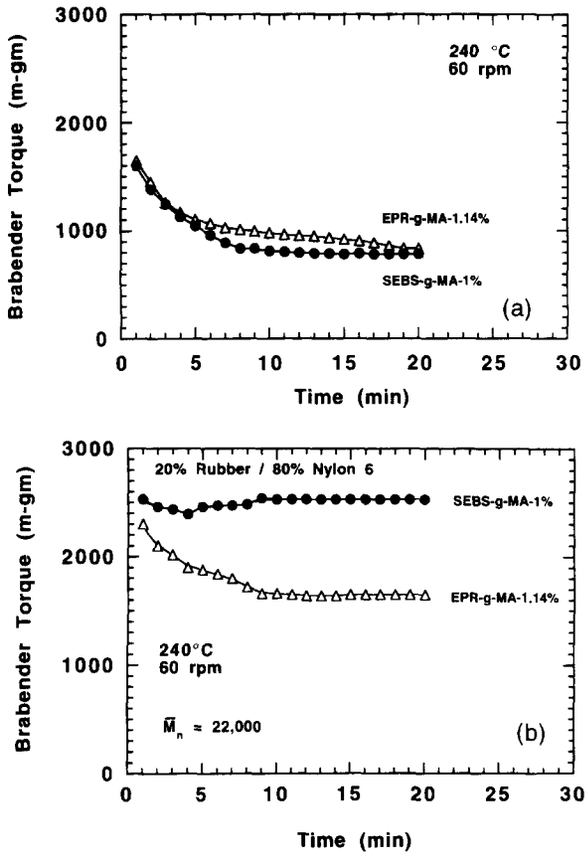

Figure 14 Brabender torque response (at 240°C and 60 rpm) for (a) EPR-g-MA and SEBS-g-MA-1% and (b) of EPR-g-MA and SEBS-g-MA-1% blends with nylon 6 have $\bar{M}_n$ = 22000 in the ratio 20% rubber/80% nylon 6

reactivity of the two rubber types, while the remaining factors will be discussed later.

Torque rheometry has frequently been used to monitor chemical reaction during reactive melt mixing[21,22,59–62]. *Figure 14a* shows the Brabender torque responses of SEBS and EPR type rubbers of similar melt viscosities and levels of maleation. However, when blended with nylon 6, the SEBS-g-MA-1% leads to a significantly greater torque value than EPR-g-MA, as seen in *Figure 14b* suggesting a greater level of reactive grafting to the former than the latter. The proposed difference in reactivity between the two maleated rubber types was explored in more detail by using the titration technique outlined earlier[50]. The amine end group content of the nylon 6 phase was determined before and after blending with the two types of rubber mixtures at different maleic anhydride contents so that the extent of amine reaction with maleic anhydride during the compounding and moulding process could be determined. The extent of amine reaction is defined as

$$\text{Extent of amine reaction} = ([NH_2]_o - [NH_2]_b)/ \times [NH_2]_o \times 100 \quad (9)$$

where the subscripts o refer to the initial amount and b to the amount after compounding and moulding. *Figure 15* shows that the extent of reaction of the SEBS/SEBS-g-MA-2% and SEBS-g-MA-*X*% materials with a medium molecular weight nylon 6 increases monotonically as the amount of maleic anhydride in the rubber phase increases; however, the EPR/EPR-g-MA mixture apparently shows a greater extent of reaction at low maleic anhydride levels and then does not change at higher levels of maleic anhydride. A similar trend was observed in the power, or electrical current readings, needed to operate the extruder at a fixed rpm[50]. *Figure 15* clearly shows that highly maleated SEBS elastomers react to a greater extent with this nylon 6 and are, therefore, more likely to produce smaller rubber particles than EPR/EPR-g-MA elastomer mixtures.

The reason for this difference in reactivity must be the result of some structural differences between the two rubber types. At this point we can only speculate on what these differences may be; however, it is useful to note some potential factors. The SEBS materials have a two phase structure since the styrene end blocks form microdomains; it is believed that maleic anhydride is grafted only to the rubbery mid-block. Thus, the local concentration of maleic anhydride is higher in this continuous phase than the overall level of maleation suggests. As shown previously, the nature of the polyamide/rubber interface can affect the extent of reaction[4,63]; it is not clear how the thermodynamic interaction between nylon 6 and these two rubber types would differ. *Figure 16* shows parallel plate rheometry data for EPR-g-MA and SEBS-g-MA-2% rubbers. While the real and imaginary moduli for the

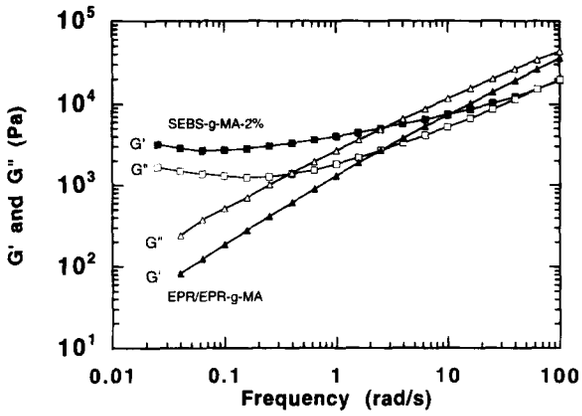

Figure 16 Viscoelastic properties (real and imaginary moduli, G′ and G″) for EPR-g-MA (triangles) and SEBS-g-MA-2% (squares) as a function of frequency at 240°C using parallel plate geometry

SEBS-g-MA-2% elastomer is higher at low shear rates, the values are lower than those for EPR-g-MA at higher shear rates. At the highest shear rate ($100\,rads^{-1}$), EPR-g-MA rubber has a melt elasticity (G') twice that of SEBS-g-MA-2%. The higher elasticity of the EPR-g-MA material at the high shear rates involved in extrusion compounding may influence the generation of surface area and, hence, the extent of interfacial reaction possible.

EFFECT OF POLYAMIDE MOLECULAR WEIGHT ON BLEND MORPHOLOGY

Other factors in addition to maleic anhydride content of the rubber phase influence the size of the rubber particles formed in blends with nylon 6, e.g. the relative and absolute rheological properties of the two phases, mixing intensity, and the extent of reaction which may be influenced by these and other factors. For a given rubber system, the mixing process has been held constant in this work. However, the molecular weight of the nylon 6 phase has been varied which influences the melt viscosity of the matrix and the number of amine groups available for reaction. *Figure 1b* shows how the melt viscosity of the nylon 6 material increases with molecular weight. Based on many correlations published in the literature[13,64–68], the melt viscosity of the matrix phase should have an important effect on the size of the dispersed particles. This issue will be addressed in a later section. The higher the molecular weight, of course, the fewer amine groups there are (see *Figure 17a*) to participate in grafting reactions; one might expect that the higher viscosity reduces the mobility needed to get the amine end groups to the interface. These factors may influence the amount of graft copolymer formed at the interface and ultimately the ability to disperse the maleated rubber in the nylon 6 matrix.

To characterize the amount of grafting that does occur, the amine concentration of the nylon 6 phase was measured before and after blending with 20% SEBS-g-MA-2%. The amine content prior to melt mixing increases linearly with the reciprocal of $\bar{M}_n$ when there is one amine per chain, see the top line in *Figure 17a*; Capron XA-1767 and Ultramid B-3 fall below the line because of their reduced amine end content due to end capping during polymerization. The amine content after melt mixing and injection moulding, the lower line in

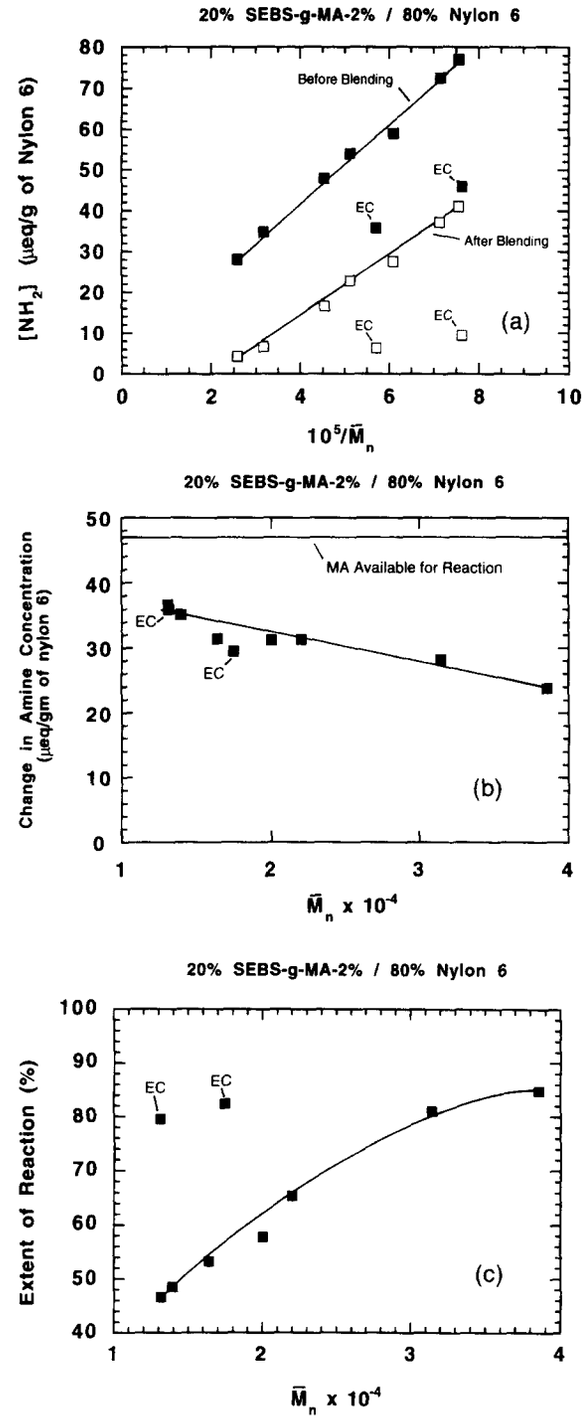

Figure 17 Effect of nylon 6 molecular weight on the amount of amine end groups, in the nylon 6 phase, that react with maleic anhydride in 20% SEBS-g-MA-2%/80% nylon 6 blends, following melt compounding and injection moulding, expressed as: (a) the concentration of amine end groups before and after melt blending, (b) the change in amine end group concentration as a result of blending, and (c) the extent of reaction as defined by equation (9). EC denotes end-capped nylon 6 materials (see *Table 1*)

Figure 17a, follows a similar trend as the initial amine content except for a different slope. The unreacted amine concentration appears to approach zero for a value of $\bar{M}_n$ of approximately $45\,000\,g\,mol^{-1}$. The amine content before and after blending for the two end capped materials fall below the trend established by the polyamides having one amine end per chain by similar amounts. The difference between the two curves in *Figure 17a* indicates the absolute amount of

amine end groups that were consumed during the blending process if certain assumptions were made. The absolute amount of amine groups that reacts during blending decreases as the molecular weight of the nylon 6 increases as seen in *Figure 17b*. For all of these compositions, there are 47 μeq of maleic anhydride available for reaction per gram of nylon 6. Thus, there is an excess of amine groups relative to anhydride except for two of the highest molecular weight polyamides and the two end capped materials. The change in amine content as a result of blending for the two end capped nylon 6 materials falls in line with all the other materials when plotted *versus* molecular weight. Because there are fewer amine end groups available for reaction as the molecular weight of nylon 6 increases, it turns out that a larger fraction of the available amine groups, as defined in equation (9), react as the nylon 6 molecular weight increases as shown in *Figure 17c*.

In addition to the grafting caused by the reaction of amine end groups with maleic anhydride on the rubber to form imide linkages, other reactions may occur. Each grafting reaction produces a water molecule which can react with amide linkages to cause chain scission if it is not removed from the extruder. In addition, acid and amine ends may react and increase the polyamide molecular weight. These reactions produce or consume, respectively, amine groups. Marechal *et al.*[49] have recently shown in model experiments using nylon 6 and low molecular weight anhydrides that hydrolysis and condensation reactions only become significant at long mixing times (>10 mn). Initially, the amine end group concentration decreases by reaction with anhydride. This reaction is fast and results in an imbalance of the amine and acid end group concentration from equilibrium conditions. Therefore, at long mixing times the equilibrium is re-established by hydrolysis. However, measurements after the various melt processing steps using a medium molecular weight nylon 6 (8207F) has shown that the amine content decreases by approximately 6% due to condensation reactions or thermal degradation. This value may increase with decreasing nylon 6 molecular weight owing to the higher concentration of end groups. Low molecular weight nylon 6 materials are known to polymerize in the solid state at elevated temperatures[32,33]. However, the mixing times used here are short compared to those needed for the side reactions of hydrolysis or condensation to be significant as shown by Marechal *et al.*[49]. On this basis, the loss of amine groups can be directly related to imide linkages or graft fraction. The extent of amine reaction as defined in equation (9) is then the fraction of the nylon 6 chains that are grafted to the rubber phase, in the case of nylon 6 materials with one amine and one acid per chain. The two end capped nylon 6 materials have extremely high extents of reaction considering the reduced number of polymer chains that can participate in the reaction. However, as seen in *Figure 17b*, the absolute amount of amine groups that react in these materials is the same as for the non-end capped nylon 6 materials of equivalent molecular weight. The fact that the same number of grafted nylon chains are formed in each case helps explain why the end capped materials have nearly identical rubber particle size and distribution as the non-end capped nylon 6 materials. For the non-end capped nylon 6 materials, the fraction of polyamide chains grafted to the rubber phase increases monotonically as the nylon 6 molecular weight increases. The higher degree of grafting combined with the high melt viscosity, which generates greater stress on the rubber phase during dispersion, evidently results in smaller rubber particle sizes with lower polydispersity.

CORRELATION OF AVERAGE PARTICLE SIZE

The morphology of a two phase blend is the result of the balance between the processes of particle break-up and coalescence[26,68–72]. Based on Taylor's theory for Newtonian fluids in a shear field, drop break-up will occur when the ratio of viscous to interfacial forces exceeds a critical value which is a function of the relative viscosities of the two phases. These principles have been used to describe dispersion phenomena that occur within flow fields for polymer blends. Correlations of the following form have been developed:

$$\eta_m G d/\gamma = F(\eta_d/\eta_m) \tag{10}$$

where γ is the interfacial tension, G is the shear rate, η_m the viscosity of the matrix phase and η_d the viscosity of the dispersed phase. The quantity on the left in equation (10) has been referred to as the capillary number (some references refer to this as the Weber number). Using models based on Smoluchowski's theory of aqueous colloid suspensions, attempts have been made to correlate the effects of coalescence on the size of particles formed[26,73,74]. These theories predict that the dispersed phase particle size increases with concentration due to the greater probability of collisions as the number of particles increases[26,75,76].

From equation (10) it is clear that the interfacial tension between the two phases is a critical factor in determining the particle size in polymer blends[77,78]. As a result, there has been considerable theoretical and experimental interest in the interfacial tension between polymer–polymer pairs[79–83]. However, at this time, it is a formidable problem to obtain any measurement or prediction of this quantity for a reactive interface where a graft copolymer is generated *in situ*. Reactions at the interface are expected to lead to a reduction in the interfacial tension, but their effect on stabilization against coalescence may be a more important consequence in blend morphology development[4,26]. Furthermore, such grafting reactions increase the viscosity of the mixture, or the level of stress when rotational speed of the mixing device is held constant, which tends to reduce particle size as may be seen from equation (10).

Numerous studies have attempted to unify data on particle size for various polymer systems, in the form suggested by equation (10), with some success. In non-reactive, immiscible polymer systems, a broad minimum in the capillary or Weber number has been observed for viscosity ratios between 0.1 and 1[65–68,71,72]. Wu has developed, for reactive and non-reactive rubbers melt blended with polyester and nylon 6,6 matrices, a master curve that shows a sharp minimum at a viscosity ratio of one[13]. This implies that the smallest particles are formed, in reactive and non-reactive systems alike, when the viscosities of the matrix and dispersed phases are equal. For reactive systems, the viscosities refer presumably to those of the original components prior to any reaction. In what follows, we use the Brabender torque, T, at a fixed rpm to characterize the rheological properties of the pure rubber and pure polyamide phases since more

detailed rheological information is not available and the Brabender does provide a deformation field not unlike that in the extruder.

We attempt here to unify the current data in the form suggested by equation (10); however, some modifications to the capillary or Weber number are made as follows. All the blends in this study were prepared under identical conditions in a single screw extruder with a high intensity mixing screw. The stresses imposed on a dispersed phase within an extruder arise from a combination of complex shear and elongational flow fields. Thus, quantifying the intensity of mixing in an extruder is not so simple as estimating an effective shear rate since this is not a well-defined quantity, but in any case the kinematics of the mixing process used have been held constant here. Thus, for simplicity, we regard the shear rate in equation (10) as a constant. As discussed earlier, the interfacial tension is a difficult parameter to determine even for non-reactive systems and must be regarded as unknown for reactive systems. The interfacial tension will obviously vary according to the extent of reaction in the present blends. We deal with this factor by defining empirical shift factors as explained below. In consideration of the above issues, equation (10) can be transformed into the following:

$$(\alpha\beta)\bar{d}_w T_{\text{Nylon 6}} = F(T_{\text{Rubber}}/T_{\text{Nylon 6}}) \qquad (11)$$

where $\bar{d}_w$ is the weight average rubber particle size, T_{Rubber} and $T_{\text{Nylon 6}}$ are the Brabender torque values of the rubber and nylon phase measured at 60 rpm and 240°C, and α and β are shift factors (defined more fully below) that account for the effective mixing intensity in the extruder, the interfacial surface tension of the blend system in the reacted state, increases in stress due to grafting reactions, and issues related to coalescence rate. An example of this modified Taylor theory analysis, prior to applying shift factors, is shown in *Figure 18* for blends of the SEBS and SEBS-g-MA-X% elastomers with the various molecular weight nylon 6 materials. It is apparent that each curve has a similar shape and slope; i.e. the curves are merely vertically displaced from one another to an extent that reflects the amount of maleic anhydride in the rubber. Thus, a master curve can be generated by selecting a reference curve and shifting the other curves to this reference.

The non-maleated SEBS curve was chosen as the reference, and the curve for each maleated rubber was shifted until it coincided with the SEBS reference curve. The magnitude of this shift on a logarithmic scale defines the multiplier or overall shift factor, $\alpha\beta$, required to achieve vertical superposition. The overall shift factor can be further divided into shift factors corresponding to the rubber type, α, and the maleic anhydride content in the rubber phase, β. That is, β is the value for shifting a maleated rubber curve to its non-maleated counterpart, SEBS or EPR. For example, multiplying each data point on the SEBS-g-MA-2% curve by the appropriate factor, $\beta = 65$, gives superposition onto the SEBS curve. The factor α, associated with the rubber type, allows the EPR/EPR-g-MA rubber system to be shifted to the SEBS reference curve. Multiplying the data points on the EPR curve by $\alpha_{\text{EPR}} = 2.8$ provides the best superposition onto the SEBS curve. The values of α_{SEBS} and β_{SEBS} are unity since the SEBS curve has been chosen as the reference. For L-SEBS-g-MA, only the overall shift factor, $\alpha\beta$, could be

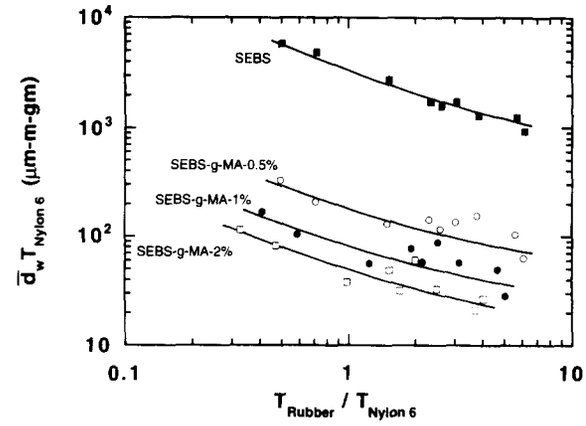

Figure 18 Modified Weber number analysis for 20% SEBS-g-MA-X%/80% nylon 6 blends as a function of the melt viscosity ratio for the rubber phase to the nylon 6 phase. Melt viscosity determined from Brabender torque response after 10 min at 240°C and 60 rpm

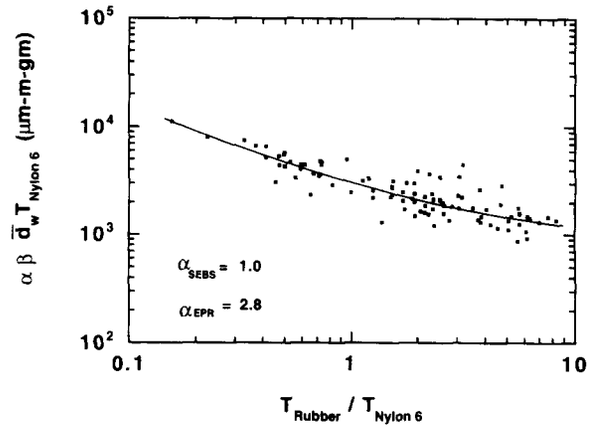

Figure 19 Modified Weber number analysis master curve using shift factors to effect superposition of the maleated rubber curves on the non-maleated reference curve, SEBS

determined since no non-maleated precursor was available for this study.

This procedure, using SEBS as the reference, leads to the master curve shown in *Figure 19*. There appears to be good correlation among the data suggesting that a unification of the rubber particle size influenced by the numerous chemical and physical parameters is possible. It is evident that there is no minimum at a viscosity ratio of unity as suggested by Wu [13], even for the non-maleated rubbers, SEBS and EPR. The overall shift factor, $\alpha\beta$, in equation (11) physically represents a combination of the shear rate (a constant), the interfacial surface tension and any factors not explicitly considered in the theory (equation (10)) such as changes in the coalescence process. The interfacial tension and coalescence rate are expected to decrease as the amount of grafting of the nylon 6 to the rubber phase increases with maleic anhydride content. Therefore, the overall shift factor should be a strongly increasing function of the maleic anhydride content of the rubber as shown in *Figure 20*. Each rubber system shows a remarkable linear correlation between the overall shift factor and the maleic anhydride content. The larger the shift factor the smaller the rubber particles. Thus, the large shift factors for SEBS-g-MA-X%'s lead to the smallest rubber particle sizes due to their efficiency to react and reduce the interfacial tension and coalescence rate. The effect

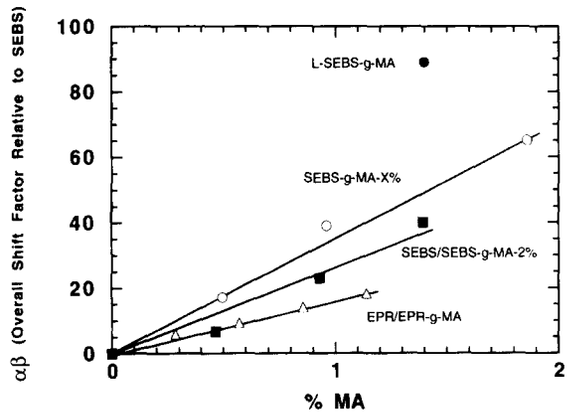

Figure 20 Overall shift factors for 20% rubber/80% nylon 6 blends as a funtion of maleic anhydride content

of the viscosity ratio on the Weber number relative to nylon 6 molecular weight appears to be constant since the slopes of all the curves are nearly identical. The data scatter at high viscosity ratios, i.e. the low molecular weight nylon 6 materials at low maleic anhydride contents, may suggest that the grafting reaction is not enough to reduce the rubber particle size and that viscosity effects are still important in morphology generation.

CONCLUSIONS

The morphology of rubber toughened nylon 6 blends has been investigated to determine the effect of nylon 6 molecular weight. By varying the molecular weight of the nylon 6 phase, the melt viscosity of the matrix and the number of amine end groups available for reaction are affected; both influence the shape, size, and size distribution of the rubber phase. As the molecular weight of the nylon 6 phase increases, both the rubber particle size and the amount of occluded material in the rubber phase decreases. Analysis of amine group content before and after blending revealed that the higher the molecular weight of the nylon 6 phase the higher the fraction of nylon 6 chains that are grafted to the rubber phase. This effect plus the higher melt viscosity, or stress on the rubber particles, explains the reduction in rubber particle size as the molecular weight of the nylon 6 increases. The weight average rubber particle size formed by SEBS-g-MA-*X*% elastomers follows the same trend as a function of maleic anhydride content found for SEBS/SEBS-g-MA-2% mixtures. However, both the average particle size and size distribution for the SEBS/SEBS-g-MA-2% mixtures are larger than the corresponding quantities for the uniformly maleated SEBS-g-MA-*X*% type elastomers. Mixtures of EPR/EPR-g-MA rubbers produce morphologies that are more complex than the SEBS type elastomers, resulting in rubber particle sizes and distributions that are typically larger and more polydisperse. Even at equivalent maleic anhydride content and melt viscosity, EPR-g-MA produces rubber particles that are much larger than those formed from an SEBS-g-MA-*X*% type elastomer. In part, this stems from the observation that SEBS elastomers react more readily with the nylon 6 than do EPR/EPR-g-MA mixtures as measured by torque rheometry and by amine end group analysis.

A modified Taylor theory analysis was found to correlate weight average rubber particle sizes for the various rubber types in nylon 6 materials of different molecular weights. A master curve was generated by determining the shift factors needed to vertically superimpose the maleated rubber/nylon 6 curves onto a reference curve for the non-maleated rubber, SEBS. The overall shift factors, which represent the effects of shear rate, the interfacial tension, changes in stress level due to graft reactions, and factors not considered by the Taylor theory, correlate linearly with the maleic anhydride content of the rubber phase.

ACKNOWLEDGEMENTS

This research was supported by the US Army Research Office. The authors would like to thank Allied-Signal Inc., Exxon Chemical Co., and Shell Development Co. for the materials and technical communications. A special thanks is made to Dr Auto Ilg and Keith Gannon of the BASF Corp. for the materials developed specifically for this study. The authors would also like to thank Dr Biswaroop Majumdar for his contributions in the area of transmission electron microscopy.

REFERENCES

1 Abbate, M., Di Liello, V., Martuscelli, E., Musto, P., Rgaosta, G. and Scarinzi, G. *Polymer* 1992, **33**, 2940
2 Martuscelli, E., Riva, F., Selitti, C. and Silvestre, C. *Polymer* 1985, **26**, 270
3 Greco, R., Malinconico, M., Martuscelli, E., Ragosta, G. and Scarinzi, G. *Polymer* 1987, **28**, 1185
4 Majumdar, B., Keskkula, H. and Paul, D. R. *Polymer* 1994, **35**, 1386
5 Lawson, D. F., Hergenrother, W. L. and Matlock, M. G. *J. Appl. Polym. Sci.* 1990, **39**, 2331
6 Ban, L. L., Doyle, M. J., Disko, M. M. and Smith, G. R. *Polym. Commun.* 1988, **29**, 163
7 Flexman, E. A. *Polym. Eng. Sci.* 1979, **19**, 564
8 Gilmore, D. W. and Modic, M. J. *Plast. Eng.* 1989, April 29
9 Modic, M. J., Gilmore, D. W. and Kirkpatrick, J. P., Proc. First. Int. Cong. on Compatibilization and Reactive Polymer Alloying (Compalloy '89), New Orleans, LA, 1989, p. 197
10 Gelles, B., Modic, M. and Kirkpatrick, J. *Soc. Plast. Eng., ANTEC* 1988, **46**, 513
11 Gilmore, D. and Modic, M. *J. Soc. Plast. Eng., ANTEC* 1989, **47**, 1371
12 Modic, M. J. and Pottick, L. A. *Plast. Eng.* 1991, **7**, 37
13 Wu, S. *Polym. Eng. Sci.* 1987, **27**, 335
14 Wu, S. *Polymer* 1985, **26**, 1855
15 Wu, C. J., Kuo, J. F. and Chen, C. Y. *Polym. Eng. Sci.* 1993, **33**, 1329
16 Wu, C. J., Kuo, J. F., Chen, C. Y. and Woo, E. *J. Appl. Polym. Sci.* 1994, **52**, 1695
17 Borggreve, R. J. M. and Gaymans, R. J. *Polymer* 1989, **30**, 63
18 Dijkstra, K., ter Laak, J. and Gaymans, R. J. *Polymer* 1994, **35**, 315
19 Dijkstra, K., Wevers, H. H. and Gaymans, R. J. *Polymer* 1994, **35**, 323
20 Dijkstra, K. and Gaymans, R. J. *Polymer* 1994, **35**, 332
21 Oshinski, A. J., Keskkula, H. and Paul, D. R. *Polymer* 1992, **33**, 268
22 Oshinki, A. J., Keskkula, H. and Paul, D. R. *Polymer* 1992, **33**, 284
23 Fayt, R., Jerome, R. and Teyssie, R. *ACS Symp. Ser.* 1989, **395**, 38
24 Lambla, M., Yu, R. X. and Lorek, S. *ACS Symp. Ser.* 1989, **385**, 67
25 Cimmino, S., Coppola, F., D'Orazio, L., Greco, R., Maglio, G., Malinconinco, M., Mancarella, C., Martuscelli, E. and Ragosta, G. *Polymer* 1986, **27**, 1874

26 Sundararaj, U. and Macosko, C. W. *Macromolecules* 1995, **28**, 2647
27 Oostenbrink, A. J., Molenaar, L. J. and Gaymans, R. J. Polyamide-rubber blends: influence of very small rubber particle sizes on impact strength, Poster given at 6th Annual Meeting of Polymer Processing Society, Nice, France, 18–20 April 1990
28 Borggreve, R. J. M., Gaymans, R. J. and Schuijer, J. *Polymer* 1989, **30**, 71
29 Borggreve, R. J. M., Gaymans, R. J., Schuijer, J. and Ingen Housz, J. F. *Polymer* 1987, **28**, 1489
30 Oshinski, A. J., Keskkula, H. and Paul, D. R. *Polymer* 1996, **37**, 4909.
31 Oshinski, A. J., Keskkula, H. and Paul, D. R. *Polymer* 1996, **37**, 4919.
32 Gilmore, P. personal communication, 1993
33 Ilg, A. personal communication, 1993
34 Takeda, Y., Keskkula, H. and Paul, D. R. *Polymer* 1992, **33**, 3173
35 Hansen, D. personal communication, 1993
36 Bach, G. 'Qualitative Methods in Morphology', Springer, Berlin, 1967
37 Irani, R. R. and Callis, C. F. 'Particle Size: Measurement, Interpretation and Application', J. Wiley and Sons, New York, 1963
38 Chamot, E. M. and Mason, C. W. 'Handbook of Chemical Microscopy', Wiley, London, 1983
39 Kohan, M. I. 'Nylon Plastics', J. Wiley and Sons, New York, 1977
40 Urbanski, J., Czerwinski, W., Janicka, K., Majewska, F. and Zowall, H. 'Handbook of Analysis of Synthetic Polymers and Plastics', J. Wiley and Sons, New York, 1972
41 Allied Signal Inc., Internal Publication, 'Analytical Sciences at Allied Signal', 1988, p. 93
42 Mason, C. D., U.S. Patent 4,945,129, 1990
43 Reimschuessel, H. K. and Dege, G. J. *J. Polym. Sci.: Part A-1* 1971, **9**, 2342
44 Zimmerman, J. in 'Encyclopedia of Polymer Science and Engineering' (Eds Mark, Bikales, Overberger and Menges), Wiley-Interscience, New York, 2nd Ed, 1988, Vol. 11, p. 353
45 Putscher, R. E., in 'Encyclopedia of Chemical Technology' (Eds Kirk and Othmer), Wiley-Interscience, New York, 3rd Edn., 1982, Vol. 18, p. 328
46 Burke, J. J. and Orofino, T. A. *J. Polym. Sci., Part A-2* 1969, **7**, 1
47 Waltz, J. E. and Taylor, G. B. *Anal. Chem.* 1947, **19**, 448
48 Tuzar, Z. and Kratochvil, P. *J. Polym. Sci., Polym. Lett. Ed.* 1965, **3**, 17
49 Marechal, P., Coppens, G., Legras, R. and Dekoninck, J. M. *J. Polym. Sci.: Part A: Polym. Chem.* 1995, **33**, 757
50 Oshinski, A. J. Ph.D. Thesis, University of Texas at Austin, 1995
51 Marechal, Ph., Legras, R. and Dekoninck, J. *J. Polym. Sci.: Part A; Polym. Chem.* 1993, **31**, 2057
52 Favis, B. D. *Canad. J. Chem. Eng.* 1991, **69**, 619
53 Dijkstra, K. Ph.D. Dissertation, University of Twente, 1993
54 Oshinski, A. J. M.S. Thesis, University of Texas at Austin, 1990
55 González-Montiel, A., Keskkula, H. and Paul, D. R. *J. Polym. Sci. Part B: Polym. Phys.* 1995, **35**, 1751
56 Majumdar, B., Keskkula, H. and Paul, D. R. *J. Appl. Poly. Sci.* 1994, **54**, 339
57 Modic, M. and Pottick, L. *Plast. Eng.* 1991, **7**, 37
58 Maier, C., Lambla, M.and Ilham, K. *ANTEC* 1995, **53**, 2015
59 Fowler, M. W. and Baker, W. E. *Polym. Eng. Sci.* 1988, Mid-Nov., **28**, 21
60 Baker, R. E. and Saleem, M. *Polymer* 1987, **28**, 2057
61 Triacca, V. J., Ziaee, S., Barlow, J. W., Keskkula, H. and Paul, D. R. *Polymer* 1991, **32**, 1401
62 Barlow, J. W., Shaver, G. P. and Paul, D. R. Proc. First International Congress on Compatibilizers and Reactive Polymer Alloying (Compalloy '89), New Orleans, LA, 1989, p. 221
63 Paul, D. R. *Macromol. Symp.* 1994, **78**, 83
64 Jordhamo, G. M., Manso, J. A. and Sperling, L. H. *Polym. Eng. Sci.* 1986, **26**, 517
65 Favis, B. D. and Chalifoux, J. P. *Polym. Eng. Sci.* 1987, **27**, 1591
66 Favis, B. D. and Willis, J. M. *J. Polym. Sci., B* 1990, **28**, 2259
67 Favis, B. D., Chalifoux, J. P. and Van Gheluwe, P. *Soc. Plast. Eng., ANTEC* 1987, 169
68 Serpe, G., Jarrin, J. and Dawans, F. *Polym. Eng. Sci.* 1990, **30**, 553
69 Dagli, S. S., Xanthos, M. and Biesenberger, J. A. Compalloy 1991, Proc. Fourth International Congress on Compatibilizers and Reactive Polymer Alloying, New Orleans, LA, 1991, 257
70 Padwa, A. *Polym. Eng. Sci.* 1992, **32**, 1703
71 Taylor, G. I. *Proc. R. Soc. Lond. (A)* 1954, **226**, 34
72 Grace, H. P. *Chem. Eng. Commun.* 1982, **14**, 225
73 Von Smoluchowski, M. *Z. Physik Chem.* 1917, **92**, 129
74 Von Smoluchowski, M. *Physik Z.* 1916, **17**, 557, 585
75 Tokita, N. *Rub. Chem. Tech.* 1977, **50**, 292
76 Forteiny, I. and Kovar, *J. Polym. Compos.* 1988, **9**, 119
77 Min, K., White, J. L., and Fellers, J. F. *Polym. Eng. Sci.* 1984, **24**, 1327
78 Chen, C. C. and White, J. L. *Polym. Eng. Sci.* 1993 , **33**, 923
79 Helfand, E. *J. Chem. Phys.* 1975, **62**, 999
80 Helfand, E. and Sapse, A. M. *J. Chem. Phys.* 1975, **62**, 1327
81 Helfand, E. and Tagami, Y. *J. Chem. Phys.* 1972, **56**, 3592
82 Anastasiadis, S. H., Gancarz, I. and Koberstein, J. T. *Macromolecules* 1988, **21**, 2980
83 Wu, S. 'Polymer Interface and Adhesion', Marcel Dekker, New York, 1982